Physica A 630 (2023) 129296

Contents lists available at ScienceDirect

Physica A

journal homepage: www.elsevier.com/locate/physa

A tensor renormalization group analysis of the Blume–Capel model inspired by game theory

Balázs Király

Institute of Technical Physics and Materials Science, HUN-REN Centre for Energy Research, Konkoly-Thege Miklós út 29–33., H-1525, Budapest, Hungary

ARTICLE INFO

Keywords:
Blume–Capel model
Elementary coordination game
Tensor renormalization group
Phase transition
Lattice spin model
Evolutionary game theory

ABSTRACT

After showing that it can be parametrized as the elementary coordination game of evolutionary game theory, this paper analyzes the Blume–Capel model using the tensor renormalization group method introduced by Michael Levin and Cody P. Nave. The results obtained along the cross sections defined by the coordination game parametrization expand and corroborate earlier findings regarding the location, order, and critical properties of the order–disorder phase transitions in both the zero-field and non-zero-field versions of the Blume–Capel model.

1. Introduction

The Blume–Capel model was originally introduced to discuss the possibility of first-order magnetic phase transitions arising as a consequence of the zero-field splitting of triplet levels of magnetic ions [1–4]. The model consists of Ising spins subject to bilinear exchange interactions and an external magnetic field and vacancies whose density is controlled by the level splitting [5]. The corresponding Hamiltonian reads

$$H = -J \sum_{\langle i,j \rangle} \sigma_i \sigma_j + \Delta \sum_i \sigma_i^2 - h \sum_i \sigma_i, \tag{1}$$

where the summation runs over all interacting site pairs $\langle i, j \rangle$, J is the exchange parameter defining the interaction between Ising spin states $\sigma_i = \pm 1$, h is the external magnetic field, $\sigma_i = 0$ represents a vacancy at site i, and Δ is the crystal-field coupling. In the following, we consider the ferromagnetic, $J > 0$ version of this model on a two-dimensional square lattice with nearest-neighbor interactions.

The Blume–Capel model has been extensively studied using a variety of different methods including, as listed with further references in Refs. [5] and [6], mean-field approximation, Monte Carlo simulations and Monte Carlo renormalization group analysis, epsilon expansions, high- and low-temperature series expansions, and phenomenological finite-size scaling.

In the zero-magnetic-field case, the system is in a ferromagnetic ordered phase dominated by aligned $+1$ or -1 spins at low temperatures and low crystal fields. Increasing the temperature disorders and increasing the crystal field dilutes this arrangement, which both can eventually drive the system into its paramagnetic phase, albeit through different kinds of transitions. Phase transitions at higher temperatures and lower crystal fields are continuous and expected to belong to the Ising universality class, whereas phase transitions occurring at lower temperatures and higher crystal fields are discontinuous, first-order transitions; these two phase boundaries meet in a tricritical point [5]. The phase diagram is shown in Fig. 1.

The presence of an external magnetic field explicitly breaks the symmetry of the two Ising spin states and alters the behavior of the system: The continuous phase transitions are smoothed out. The first-order transitions, on the other hand, are only shifted in

E-mail address: kiraly.balazs@ek.hun-ren.hu.

https://doi.org/10.1016/j.physa.2023.129296
Received 7 August 2023; Received in revised form 7 October 2023
Available online 14 October 2023

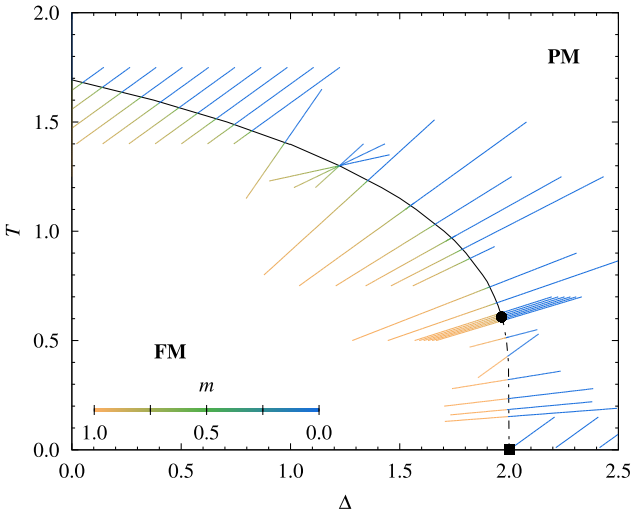

Fig. 1. Heat map of the magnetization along elementary coordination game cross sections of the Blume–Capel model according to TRG results obtained for $\chi_{\text{cut}} = 14$ and $R = 22$ iterations. From left to right $n = 6, h'' = 0.57, 0.54, \ldots, 0.30$; $n = 4, h'' = 0$; $n = 100, h'' = 1.1841$; $n = 10, h'' = 0.3698$; $n = 5, h'' = 0.051$; $n = 5, 6, \ldots, 10, 15, 20, 25, 26, \ldots, 30, 50, h'' = 0$; $n = 6, h'' = -0.35$; $n = 500, 5000, 50000, 500000, h'' = 0$; and $n = 6, h'' = -0.50, -0.55, -0.60$. The solid and dash-dotted lines indicate the continuous and first-order phase transition boundaries (separated by a tricritical point at the black dot) of the zero-field Blume–Capel model. The data used to draw the phase boundary were taken from Ref. [5], which compiles data from Refs. [5,7–10].

location to a higher transition temperature while remaining of the first-order as long as the external magnetic field is not too strong; they become continuous at a (crystal-field-dependent) critical magnetic field strength; and the system exhibits no phase transitions for larger magnetic fields [11,12].

The Blume–Capel model is paradigmatic not only in condensed matter physics but also in game theory. To better understand why this is the case, we should take a step back and first look at the connection between evolutionary game theory and the classical spin models of statistical physics.

2. The equivalence of the Blume–Capel model and the elementary coordination game

In game theory [13], pair interactions where players have a finite set of strategies to independently choose from are typically defined through so-called payoff matrices, which simply tabulate the possible outcomes. When the players are identical in the sense that they have the same strategy set and they trade payoffs when they trade strategy choices, the game is called symmetric and it can be defined by a single square matrix. On the analogy of vectors, any matrix can also be considered as a linear combination of a set of basis matrices [14]. It turns out that there exists a basis which consists of just four fundamentally different kinds of elementary matrices that each describe archetypal game situations: self- and cross-dependent games, where a player's payoff is determined solely by their own or their opponent's strategy choice; coordination games, which reward players choosing the same strategy; and rock–paper–scissors-like cyclic dominance games. With the help of this decomposition, one can readily identify matrix games with an important property: Those, and only those, symmetric matrix games are potential games (i.e., games in which the incentives of all players to unilaterally change their strategy can be expressed using a single function) that have a vanishing cyclic component [14].

Consider the following, rather general, repeated game [13,14]: Multiple players located at the sites of a lattice (or the nodes of a network) simultaneously play the same matrix game defined by the $n \times n$ payoff matrix $\mathbf{G}$ against all of their neighbors again and again, each having one chosen strategy at any given time they use in all of their interactions. After each round, one of the players is randomly chosen, and allowed to change their strategy according to some prescribed rule. When the pair interactions are potential games, the logit strategy update rule — which picks strategy s'_x with probability

$$w(s_x \to s'_x) = \frac{\mathrm{e}^{u_x(s'_x, s_{-x})/T}}{\sum_{s''_x} \mathrm{e}^{u_x(s''_x, s_{-x})/T}}, \tag{2}$$

where $u_x(s_x, s_{-x}) = \sum_\delta G_{s_x, s_{x+\delta}}$ is the total payoff of player x playing strategy s_x in the previous round against their opponents (playing strategy profile s_{-x}) located at neighboring sites $x+\delta$ and T is the so-called noise parameter — satisfies detailed balance with the Boltzmann distribution defined by the potential of the multiplayer game. Consequently, such a many-player iterated potential game is equivalent to the Markov chain Monte Carlo simulation of a classical spin model. The players and their strategies correspond to spins and spin states, the negative of the game's potential plays the role of the Hamiltonian (since players strive to maximize and not minimize their payoffs), and the logit rule and the noise parameter are analogous to Glauber dynamics and temperature.

The simplest non-trivial, truly interactive potential matrix game, in terms of the decomposition scheme outlined above, is the elementary coordination game [15]. In general, it consists of n strategies, of which 2 are coordinated and $n-2$ are neutral (or invisible in the parlance of a similar family of extended Potts models reviewed in Ref. [16]). The players both receive or lose 1 unit of payoff if they play matching or opposing coordinated strategies, respectively. Otherwise, if either player chooses one of the neutral strategies, neither receives any payoff. (For $n=2$, there are no neutral strategies, and the 2×2 elementary coordination game is the only non-trivial symmetric elementary matrix game. Its combinations with the 2×2 self-and cross-dependent games generate all two-strategy symmetric games, which all admit a potential. As a result, all four classes of 2×2 games – prisoner's dilemma, chicken or snowdrift, stag hunt, and trivial or harmony games – can be formulated as Ising models. This correspondence has proven extremely fruitful in the interdisciplinary study of a wide range of phenomena. For more information on 2×2 games, see, for example, Refs. [14,17–19].) Without any loss of generality, let us assume henceforth that the first two strategies are the coordinated ones. This general elementary coordination game's payoff matrix is

$$\mathbf{G}^{(\mathrm{co})}=\begin{pmatrix} -1 & 1 & 0 & \cdots & 0\\ 1 & -1 & 0 & \cdots & 0\\ 0 & 0 & 0 & \cdots & 0\\ \vdots & \vdots & \vdots & \ddots & \vdots\\ 0 & 0 & 0 & \cdots & 0 \end{pmatrix}. \tag{3}$$

As this payoff matrix provides no incentives for the spontaneous breaking of their symmetry, we can surmise that the neutral strategies will always be present in equal proportion and distributed uncorrelatedly in the system. This assumption is borne out by previous results obtained by mean-field approximation and Monte Carlo simulation [20].

Consequently, we might as well consider the neutral strategies indistinguishable and bundle or bunch them together into a single strategy. Of course, we have to do this in a way that is consistent with the dynamics of tzhe model, keeping the transition rates dictated by the logit update rule intact. For example, the probability $\widetilde{w}(\tilde{1}\to\tilde{3})$ of switching from the first coordinated strategy to the bunching strategy $\tilde{3}$ has to be equal to the total probability of switching to any of the neutral strategies in the original formulation of the elementary coordination game $\sum_{s'_x=3}^{n} w(1\to s'_x)$. It is easy to check [20,21] that these consistency conditions are satisfied if we add a temperature-dependent extra weight to the coordinated strategies in the form of a self-dependent, magnetic-field-like payoff component, as described by the payoff matrix

$$\widetilde{\mathbf{G}}^{(\mathrm{co})}=\begin{pmatrix} 1-\frac{\ln(n-2)}{z}T & -1-\frac{\ln(n-2)}{z}T & -\frac{\ln(n-2)}{z}T\\ -1-\frac{\ln(n-2)}{z}T & 1-\frac{\ln(n-2)}{z}T & -\frac{\ln(n-2)}{z}T\\ 0 & 0 & 0 \end{pmatrix}, \tag{4}$$

which through its potential defines the multiplayer Hamiltonian

$$H(n)=-\sum_{\langle x,y\rangle}\sigma_x\sigma_y+K\ln(n-2)\sum_i\sigma_i^2, \tag{5}$$

where $\sigma=-1,0,1$ represent $\tilde{s}=\tilde{2},\tilde{3},\tilde{1}$, respectively. This is clearly the (ferromagnetic, zero-field) Blume–Capel model of Eq. (1) – or, more precisely, a one-dimensional cross section of it, as Fig. 1 illustrates. (The z in the formula for $\mathbf{G}^{(\mathrm{co})}$ denotes the coordination number of the underlying regular lattice; $z=4$ for the square lattice. The same bunching procedure can be carried out on irregular lattices or networks, too, but then it leads to an asymmetric self-dependent component and, consequently, a non-uniform crystal field.)

We can trivially extend the above bunching idea to a wider family of models if we consider the elementary coordination game in the presence of an additional uniform self-dependent component of strength h'' that keeps the symmetry of both the coordinated and neutral strategies intact. The corresponding payoff matrix reads

$$\mathbf{G}^{(\mathrm{co+h''})}=\begin{pmatrix} 1+h'' & -1+h'' & h'' & \cdots & h''\\ -1+h'' & 1+h'' & h'' & \cdots & h''\\ 0 & 0 & 0 & \cdots & 0\\ \vdots & \vdots & \vdots & \ddots & \vdots\\ 0 & 0 & 0 & \cdots & 0 \end{pmatrix}. \tag{6}$$

It turns out that such an external field does not interfere with how the neutral strategies are bunched in any meaningful way, and thus it simply shifts the crystal-field coupling of the bunched version of the model by h'' according to

$$\Delta(n,h'')=T\ln(n-2)-zh''. \tag{7}$$

This equation still defines a line in the phase diagram of the Blume–Capel model, whose slope and intercept are determined by n and h''. (When applied to the $q=2$ Potts model with r additional invisible states, the same bunching process leads to similar cross sections of the Blume–Emery–Griffiths model [16,22].) Interestingly, h'' has more influence over the system's behavior even though the self-dependent component exhibits no phase transition when considered on its own [20]: Regardless of the n number of strategies, we can always find h'' self-dependent field strengths that define Blume–Capel models with one continuous phase transition or one first-order phase transition or no phase transition at all, but not vice versa.

Not only does this parametrization grant systematic access to analyzing the phase transitions of the Blume–Capel model in a much wider range of directions than usually considered (they have typically been studied along lines of constant Δ, varying only the temperature, with some exceptions [5]), it is also of relevance for game theory, as it demonstrates how the interplay of elementary game components can have non-trivial consequences in even seemingly simple compound games.

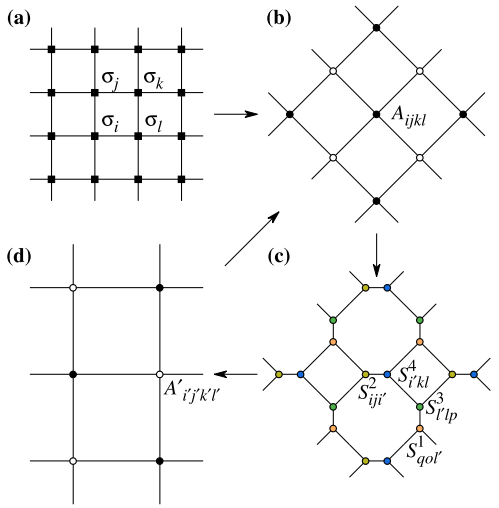

Fig. 2. Schematic drawing of the stages of the TRG method on a square lattice. The partition function of the original spin model in (a) is reformulated as the tensor network in (b), then the tensors are split in two in a checkerboard pattern via SVD to get (c), which after coarse graining yields another square-lattice tensor network (d). This allows successive iteration of the last two steps.

3. Methods

In this article, I aim to verify the above equivalence connection between the elementary coordination game and the Blume–Capel model and get a more accurate picture of their behavior in a symmetry-breaking self-dependent/magnetic field, in the hope that these results might also shed some light on the interplay between elementary games. To this end, I have studied the bunched elementary coordination game using the tensor renormalization group method (TRG) introduced by Michael Levin and Cody P. Nave [23], a method, which to my knowledge has so far only rarely been applied to the Blume–Capel model [24].

The TRG method, like a number of related methods used to study various quantum systems [25], exploits the tensor network structure of a key quantity. Specifically, it evaluates the partition function of classical spin models by recognizing said structure and systematically carrying out its contractions. Consider the lattice Hamiltonian

$$H = \sum_{\langle i,j\rangle} J^{(ij)}_{\sigma_i\sigma_j} \tag{8}$$

defined by available spin states $\sigma_i = 1...n$, coupling coefficient matrices $J^{(ij)}$, and nearest neighbor connections $\langle i,j\rangle$. On a square lattice, the tensor network structure of the corresponding partition function can be made apparent by grouping the lattice sites into four-site plaquettes $\langle i,j,k,l\rangle$ each contributing its Boltzmann weight A_{ijkl} in the following way:

$$Z = \sum_{\{\sigma\}} \mathrm{e}^{-H/T} = \sum_{\{\sigma\}} \prod_{\langle i,j\rangle} \mathrm{e}^{-J^{(ij)}_{\sigma_i\sigma_j}/T} = \sum_{\{\sigma\}} \prod_{\langle i,j,k,l\rangle} \mathrm{e}^{-\left(J^{(ij)}_{\sigma_i\sigma_j}+J^{(jk)}_{\sigma_j\sigma_k}+J^{(kl)}_{\sigma_k\sigma_l}+J^{(li)}_{\sigma_l\sigma_i}\right)/T} = \sum_{\{\sigma\}} \prod_{\langle i,j,k,l\rangle} A_{ijkl} \tag{9}$$

The actual TRG approach of calculating this sum over all $\{\sigma\}$ configurations consists of the successive iteration of a two-step coarse-graining algebraic manipulation illustrated by Fig. 2: The first step expands the tensor network by splitting the A_{ijkl} tensors in two via singular value decompositions (SVDs, u and v are unitary, s is positive diagonal)

$$A_{ijkl} = \sum_{i'=1}^{n^2} u^{\mathrm{A}}_{ili'} s^{\mathrm{A}}_{i'i'} v^{\mathrm{A}}_{i'kj} = \sum_{i'=1}^{n^2} S^1_{ili'} S^3_{i'kj} \tag{10}$$

$$A_{ijkl} = \sum_{i'=1}^{n^2} u^{\mathrm{B}}_{iji'} s^{\mathrm{B}}_{i'i'} v^{\mathrm{B}}_{i'kl} = \sum_{i'=1}^{n^2} S^2_{iji'} S^4_{i'kl} \tag{11}$$

applied in a checkerboard pattern. The second step then contracts the original index pairs, merging groups of four split tensors. The resulting tensor network has the same square lattice structure but consists of half as many $A'_{i'j'k'l'}$ tensors as the one we started out with, ensuring that the successive iterations will eventually reduce any arbitrarily large initial network to a directly manageable size. Nonetheless, calculation of the partition function still remains practically intractable for large systems without an additional interstitial approximation, since otherwise the number of singular values in the decompositions, and thus the contraction index range of the tensor network, increases exponentially with each consecutive iteration. In the original TRG algorithm proposed by Levin and Nave [23], this approximation consists of truncating the SVDs by including only the χ_{cut} largest singular values. Even though this truncated SVD is the most accurate approximation of A as a product of two tensors connected by an index of rank χ_{cut} [23,26], it does not properly account for short-range correlations, which raises some issues about the renormalization group flow analysis of its

results [26–29]. Subsequent research has developed various refinements that overcome this shortcoming [26,28–32]. Nonetheless, the simpler, original TRG algorithm applied with $\chi_{\text{cut}} = 14$ and $R = 22$ iterations proved accurate enough for the aims and scope of the present study, as attested to by the results reported in the next section.

The actual algorithm used in this article differs in just two technical details from the one described above: (i) Instead of computing extensive quantities such as energy or magnetization and quantities related to their moments (e.g., energy, specific heat, susceptibility, Binder parameter, etc.) as direct numerical derivatives of the partition function, the algorithm calculates them via numerical derivatives of the cumulant-generating functions of said quantities, each $Q = \sum_i Q_i$ of which can also be formulated using tensor networks as

$$K(a) = \ln \left\langle \mathrm{e}^{aQ} \right\rangle = \ln \left[\frac{1}{Z} \sum_{\{\sigma\}} \prod_{\langle i,j,k,l \rangle} \mathrm{e}^{a(Q_i+Q_j+Q_k+Q_l)} A_{ijkl} \right], \tag{12}$$

as described in Ref. [33]. (ii) Similar to Ref. [34], the largest W_r entry of the tensors are factored out at the beginning of each iteration step r, so that the SVD is carried out on $\overline{A}^{(r)} = A^{(r)}/W_r$ to help avoid numerical overflow. Then on an $N = 2^{3+R}$-site square lattice with uniform interactions the partition function (and similarly the moment generating functions) can be calculated as

$$Z = \prod_{r=0}^{R} W_r^{N/2^{r+1}} \sum_{\{\sigma\}} A^r_{ijkl} A^r_{mloj} A^r_{oqmp} A^r_{kqip}, \tag{13}$$

and thus each normalization factor contributes to the per site free energy (and similarly the cumulant generating functions) according to

$$f = -\frac{T}{N} \ln Z = -T \sum_{r=0}^{R} \frac{1}{2^{r+1}} \ln W_r - \frac{T}{N} \ln \sum_{\{\sigma\}} A^r_{ijkl} A^r_{mloj} A^r_{oqmp} A^r_{kqip}. \tag{14}$$

4. Results

Turning now to the bunched elementary coordination game defined by the Hamiltonian Eq. (1) and the parametrization Eq. (7), the quantities of interest are the per site averages of the free energy f; the energy $\langle H \rangle / N$; their difference divided by the temperature, the entropy s; the energy's second cumulant divided by T^2, the specific heat $c = \langle (\Delta H)^2 \rangle / (N^2 T^2)$; the difference between the frequencies of the two coordinated strategies, the Ising-type magnetization m; its second cumulant divided by the temperature, the magnetic susceptibility $\chi_{\text{m}} = \langle (\Delta m)^2 \rangle / T$; its fourth moment divided by the square of its second moment, the magnetization's Binder parameter $B_{\text{m}} = \langle m^4 \rangle / \langle m^2 \rangle^2$; the frequency of the neutral strategy/empty sites ρ_{n}; its susceptibility χ_{n}; and its Binder parameter B_{n}. The following results for these quantities obtained using the TRG method described above demonstrate both the correspondence between the elementary coordination game and the Blume–Capel model and the adequacy of the TRG method for such investigations. In order to get a fuller picture, the elementary coordination game was examined for a wide range of parameters, including sets with fixed n and varying h'', varying n and fixed h'', and varying n and varying h'' chosen in such a way that the (expected) location of the phase transition remains unchanged. The examples shown in Fig. 3 are representative of the typical observed behaviors.

When the line defined by the model parameters n and h'' crosses the solid curve in Fig. 1, the temperature dependence of the properties of the system is qualitatively similar to that seen in Figs. 3a and 3b: The free energy, the energy, and the frequency of neutral sites monotonously increase, while the entropy monotonously decreases as the temperature of the system becomes higher. The specific heat and the susceptibility (and thus the fluctuations) of the frequency of the neutral sites both have a sharp peak characterized by vanishing critical exponents from both sides at a critical temperature T_{c}. The Binder parameter of the magnetization drops from $2/3$ to 0 at the same critical temperature. The magnetization goes from 1 to 0 continuously and monotonously following a power law with critical exponent $\beta = 1/8$ as the temperature goes from 0 to T_{c}, and remains 0 above T_{c}. The susceptibility of the magnetization also follows a power law as temperature approaches the critical point from above, and after a sudden drop seems to relatively slowly increase to a plateau as the temperature decreases. These results indicate that the system undergoes a continuous order–disorder phase transition belonging to the Ising universality class in the thermodynamic limit. The non-power-law behavior of the magnetic susceptibility below the critical temperature might, at first blush, seem to contradict this conclusion, but it just reflects the fact that the TRG method takes proper account of the model's symmetry. On a finite lattice, configurations that can be transformed into each other by flipping the two coordinated strategies contribute equally to the partition function. As a result, the magnetization vanishes and its variance becomes high even at low temperatures when ordered configurations have the largest Boltzmann weights, and this degeneracy is only lifted by spontaneous symmetry breaking in the thermodynamic limit. Indeed, the finite magnetization and the peak in its susceptibility indicative of the expected phase transition were achieved using one-sided finite differences to numerically evaluate the numerical derivatives of the corresponding cumulant generating function, which in effect explicitly breaks the symmetry of the coordinated strategies.

When n is higher and/or h'' is lower, the corresponding elementary coordination game defines a cross section of the Blume–Capel model that crosses the dashed line in Fig. 1 as the temperature is varied. In these cases, the quantities mentioned above exhibit sudden jumps and seem to become discontinuous at the critical temperature indicated by the intersection of the cross section and the dashed transition line (for an example, see Fig. 3c) signaling first-order phase transitions as expected.

The boundary between the continuous and first-order transition regimes, just like the continuous transitions themselves, does not appear as entirely sharp due to the approximative nature of the TRG method, making precisely identifying the tricritical point and

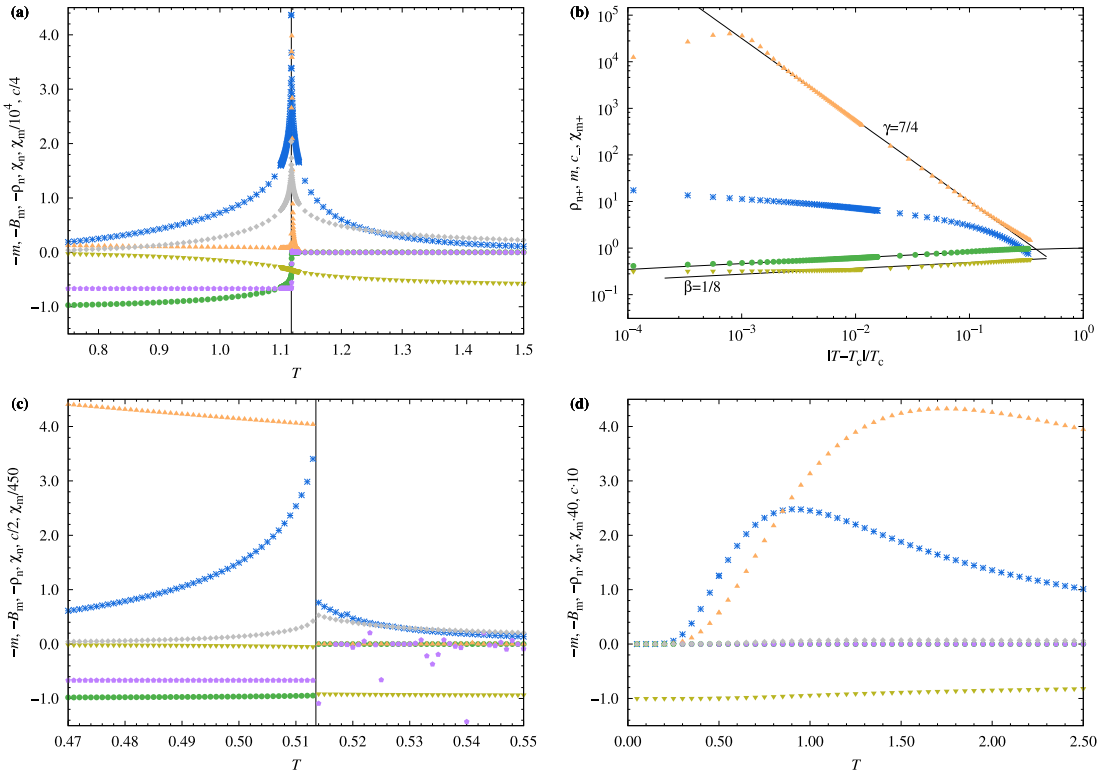

Fig. 3. Typical temperature-dependent behaviors in the Bume–Capel model/elementary coordination game as shown by the magnetization m (circles), its susceptibility χ_m (upward pointing triangles), its Binder parameter B_m (pentagons), the frequency of empty/neutral sites ρ_n (downward pointing triangles) and its susceptibility χ_n (diamonds), and the specific heat c (stars), variously rescaled for better visibility as indicated by the axis labels. In (a) and (b) $n = 6, h'' = 0$, and the system undergoes a continuous order–disorder phase transition. (c) shows a first-order phase transition when $n = 50, h'' = 0$. No phase transition occurs in (d) for $n = 6, h'' = -0.55$. The black lines in (b) represent Ising-type critical power law behavior with the indicated critical exponents. The one spanning the whole horizontal axis shows Onsager's exact results for the magnetization of the square-lattice Ising model [35]. Quantities with lower + and — indices were measured above and below the critical temperature estimated by the maximum location of the specific heat.

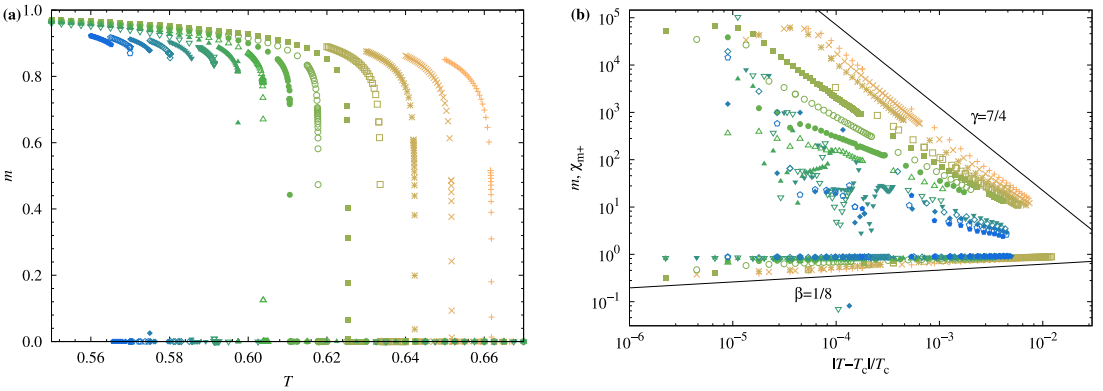

Fig. 4. The magnetization and its susceptibility near the tricritical point for $n = 21, 22, \ldots, 35$: from right to left in (a); from bottom to top (top to bottom) in (b) for the magnetization (the susceptibility). Increasing n clearly drives the transition away from Ising-type critical behavior towards jump-like first-order transitions.

classifying nearby phase transitions difficult. As n is increased towards the tricritical point ($n \approx 27.37$, h''=0; cf. [5,21]) the log–log plot of the magnetization (Fig. 4), for example, slowly shifts from being consistent with Ising-type behavior to being indicative of a jump-like transition.

When $h'' < -1/2$, forming coordinated strategy pairs no longer provides a net positive payoff, the Nash equilibrium of the multiplayer elementary coordination game (the ground state of the Blume–Capel model) becomes infinitely degenerate in the thermodynamic limit, and the system exhibits no temperature-induced order–disorder phase transition (see Fig. 3d).

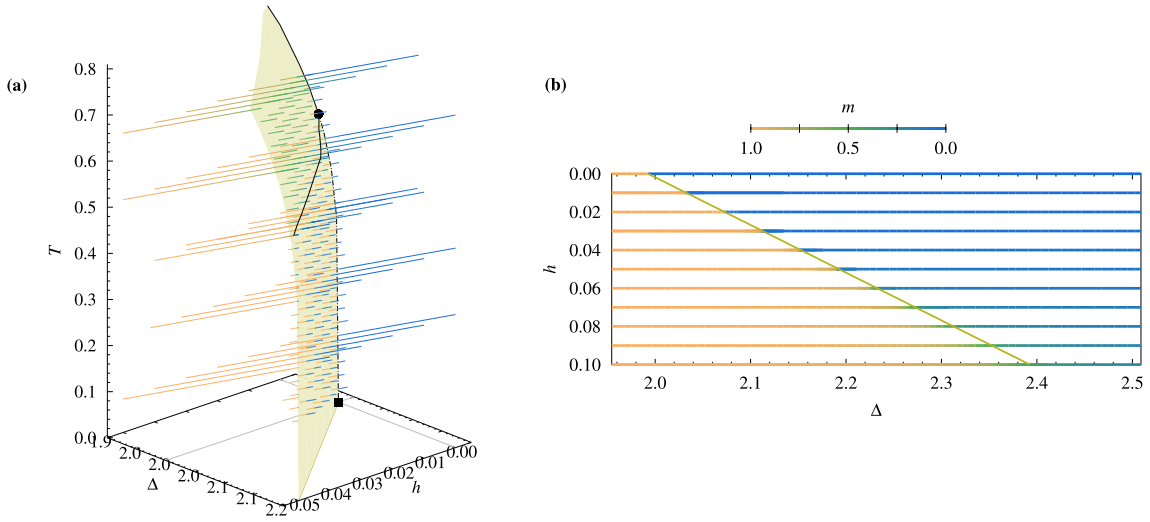

Fig. 5. (a) Three-parameter (for cross sections with $n = 6$, $h'' = -0.25, -0.26, \ldots, -0.49$) and (b) projected two-parameter ($n = 6, h'' = -0.35$) heat maps of the TRG magnetization of the Blume–Capel/elementary coordination game model in the presence of an external magnetic field h. The black phase boundary lines and dots at $h = 0$ are the same as in Fig. 1. The other solid black cure starting from the tricritical point is a rough approximation of the continuous-transition upper boundary of the first-order-transition wing based on TRG results. The yellow (middle gray) surface and line map the $h = 0$ phase boundary according to Eq. (16), which apparently provides a good estimate for the first-order phase boundary for finite h.

The results reported in this section are in excellent qualitative agreement with the literature of the Blume–Capel model [5] and also provide rather accurate approximations for quantitative details like the location (Fig. 1) and critical exponents (Figs. 3b and 6) of the phase transitions of the model. Not only do these successes prove that the elementary coordination game [Eq. (3)] and its bunched version [Eq. (15)] are indeed equivalent to the Blume–Capel model, they also show that even the simplest, least resource-intensive TRG method is capable of reliably exploring the most important features of the phase diagram of the model. The remainder of this section extends this analysis to the less well-known case of an additional external magnetic field acting on the Blume–Capel model that explicitly breaks the symmetry of its Ising states.

The bunched payoff matrix of the general elementary coordination game subject to a self-dependent component that explicitly breaks the symmetry of its coordinated strategies is

$$\widetilde{\mathbf{G}}^{(\mathrm{co+h''+}h)} = \begin{pmatrix} 1 - \frac{\Delta}{z} + h & -1 - \frac{\Delta}{z} + h & -\frac{\Delta}{z} + h \\ -1 - \frac{\Delta}{z} - h & 1 - \frac{\Delta}{z} - h & -\frac{\Delta}{z} - h \\ 0 & 0 & 0 \end{pmatrix}. \tag{15}$$

Mean-field approximation gives the following general account of the system's behavior [1–4,20]: The external magnetic field smooths out the temperature-driven continuous phase transitions of the zero-field Blume–Capel model. A first order transition is just shifted to higher critical temperatures by magnetic fields weaker than a critical value $h_c(n, h'')$; when $|h| = h_c(n, h'')$, it become continuous; while for stronger magnetic fields the phase transition vanishes. Thus, the three-dimensional phase diagram of the model consists of the zero-field phase diagram and two symmetric slanted "wings" attached to it at the line of its temperature-driven first-order transitions, as schematically shown in Refs. [11] and [12] and approximately shown in Fig. 5a based on the present TRG results. Further first-order transitions can be observed as the model parameters (n, h'', h, T) cross either the $h = 0$ plane or the two wings below their continuous transition phase boundary lines, between two oppositely ordered phases and an ordered and a disordered phase, respectively.

Applying the TRG method to the non-zero-field model lends further support to the claims of mean-field theory. The temperature-dependent behavior of the magnetization (see Fig. 5), its susceptibility, the specific heat, and the frequency and susceptibility of the neutral strategy all indicate no sharp transition above and very sharp, jump-like transitions below a symmetric pair of curved lines starting from the tricritical point. It appears that the location of these first-order transition wings is well approximated by a linear shifting of the crystal field parameter: The surface traced by mapping the points of the zero-field first-order boundary according to

$$(\Delta, 0, T) \to (\Delta + z\,|h|\,, h, \frac{\Delta + z\,|h|}{\Delta} T) \tag{16}$$

is close to the transition points predicted by the TRG method, especially away from the upper boundary of the wing, as shown by Fig. 5.

Despite their vanishing under the influence of the external magnetic field, the continuous phase transitions still inform the behavior of the Blume–Capel model in their vicinity. Results obtained with the TRG method (see Fig. 6) provide further evidence that the continuous zero-field transitions belong to the Ising universality class, as they show that at fixed critical temperatures the field-dependent magnetization follows a power law characterized by a critical exponent $\delta \approx 15$.

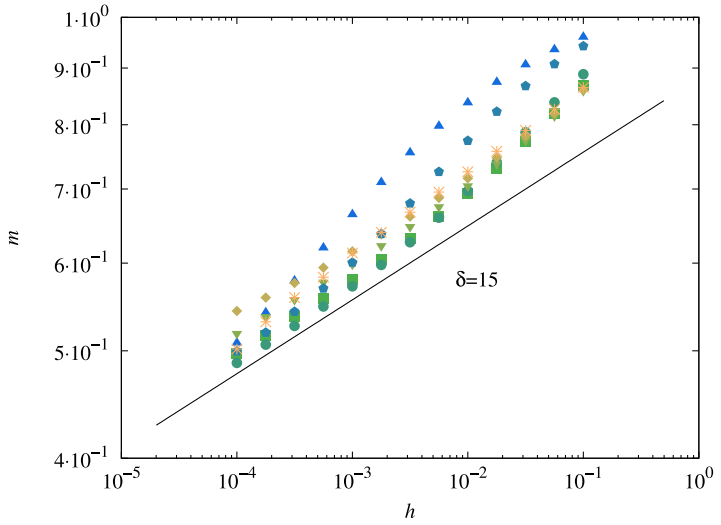

Fig. 6. Magnetic field-dependence of the magnetization at the TRG-estimated (zero-field) critical temperature and crystal field for $n = 6, h'' = 0.42, T_c = 1.57$ (stars); $n = 4, h'' = 0, T_c = 1.405$ (diamonds); $n = 5, h'' = 0.051, T_c = 1.30$ (downward pointing triangles); $n = 6, h'' = 0, T_c = 1.118$ (boxes); $n = 8, h'' = 0, T_c = 0.96925$ (circles); $n = 15, h'' = 0, T_c = 0.745$ (pentagons); $n = 20, h'' = 0, T_c = 0.6728$ (upward pointing triangles). The straight black line illustrates Ising-type power law behavior with critical exponent $\delta = 15$.

5. Summary

In this paper, I used the tensor renormalization group technique introduced by Michael Levin and Cody P. Nave to analyze the square-lattice Blume–Capel model in a parametrization that bears special relevance to game theory. Combinations of the general n-strategy elementary coordination game and a self-dependent game that maintains the symmetry of its coordinated strategies define straight-line cross-sections of the phase diagram of zero-field Blume–Capel model via a consistent bunching of the $(n - 2)$ non-coordinated neutral strategies. The results confirm the correspondence between the two models, indicate the presence of continuous and first-order order–disorder phase transitions at the expected locations, and provide further evidence that the continuous transitions belong to the Ising universality class. The TRG method proved similarly successful in describing the less well-documented case of the non-zero-field Blume–Capel model, reproducing its main qualitative features predicted by mean-field approximation while providing quantitative details consistent with Monte Carlo simulation result from the literature of the zero-field model.

CRediT authorship contribution statement

Balázs Király: Conceptualization, Methodology, Software, Formal analysis, Investigation, Visualization, Writing.

Declaration of competing interest

The authors declare that they have no known competing financial interests or personal relationships that could have appeared to influence the work reported in this paper.

Data availability

Data will be made available on request.

Acknowledgments

This work was supported by the National Research, Development and Innovation Office – NKFIH, Hungary under grant number OTKA PD-138571.

References

[1] M. Blume, Theory of the first-order magnetic phase change in UO_2, Phys. Rev. 141 (2) (1966) 517–524.
[2] H. Capel, On the possibility of first-order transitions in Ising systems of triplet ions with zero-field splitting, Physica 32 (1966) 966–988.
[3] H. Capel, On the possibility of first-order transitions in Ising systems of triplet ions with zero-field splitting II, Physica 33 (1967) 295–331.
[4] H. Capel, On the possibility of first-order transitions in Ising systems of triplet ions with zero-field splitting III, Physica 37 (1967) 423–441.
[5] J. Zierenberg, N. Fytas, M. Weigel, W. Janke, A. Malakis, Scaling and universality in the phase diagram of the 2D Blume–Capel model, Eur. Phys. J. Spec. Top. 226 (2017) 789–804.
[6] J. Plascak, J. Moreira, F. Sá Barreto, Mean field solution of the general spin Blume–Capel model, Phys. Lett. A 173 (1993) 360.
[7] P. Beale, Finite-size scaling study of the two-dimensional Blume–Capel model, Phys. Rev. B 33 (3) (1986) 1717–1720.
[8] C. Silva, A. Caparica, J. Plascak, Wang–Landau Monte Carlo simulation of the Blume–Capel model, Phys. Rev. E 73 (2006) 036702.
[9] A. Malakis, A. Berker, I. Hadjiagapiou, N. Fytas, T. Papakonstantinou, Multicritical points and crossover mediating the strong violation of universality: Wang–Landau determinations in the random-bond $d = 2$ Blume–Capel model, Phys. Rev. E 81 (2010) 041113.
[10] W. Kwak, J. Jeong, J. Lee, D.-H. Kim, First-order phase transition and tricritical scaling behavior of the Blume–Capel model: A Wang–Landau sampling approach, Phys. Rev. E 92 (2015) 022134.
[11] D. Dias, F. Lima, J. Plascak, Generalized Gibbs phase rule and multicriticality applied to magnetic systems, Entropy 24 (2022) 63.
[12] E. Albano, M. Bab, G. Baglietto, R. Borzi, T. Grigera, E. Loscar, D. Rodríguez, M. Rubio Puzzo, G. Saracco, Study of phase transitions from short-time non-equilibrium behaviour, Rep. Progr. Phys. 74 (2011) 026501.
[13] G. Szabó, G. Fáth, Evolutionary games on graphs, Phys. Rep. 446 (2007) 97–216.
[14] G. Szabó, I. Borsos, Evolutionary potential games on lattices, Phys. Rep. 624 (2016) 1–60.
[15] G. Szabó, B. Király, Extension of a spatial evolutionary coordination game with neutral options, Phys. Rev. E 93 (2016) 052108.
[16] M. Krasnytska, P. Sarkanych, B. Berche, Y. Holovatch, R. Kenna, Potts model with invisible states: A review, Eur. Phys. J. Spec. Top. (2023) http://dx.doi.org/10.1140/epjs/s11734-023-00843-3.
[17] S. Galam, B. Walliser, Ising model versus normal form game, Physica A 389 (2010) 481–489.
[18] J. Tanimoto, Fundamentals of evolutionary game theory and its applications, in: Evolutionary Economics and Social Complexity Science, vol. 6, Springer, Tokyo, 2015.
[19] J. Tanimoto, Sociophysics approach to epidemics, in: Evolutionary Economics and Social Complexity Science, vol. 23, Springer, Tokyo, 2021.
[20] B. Király, G. Szabó, Evolutionary games with coordination and self-dependent interactions, Phys. Rev. E 95 (2017) 012303.
[21] B. Király, Phase Transitions in Evolutionary Potential Games (Ph.D. thesis), Budapest University of Technology and Economics, 2019.
[22] R. Tamura, S. Tanaka, N. Kawashima, Phase transition in Potts model with invisible states, Progr. Theoret. Phys. 124 (2) (2010) 381–388.
[23] M. Levin, C. Nave, Tensor renormalization group approach to two-dimensional classical lattice models, Phys. Rev. Lett. 99 (2007) 120601.
[24] J. Osorio Iregui, Connecting the Dots: Tensor Network Algorithms for Two-Dimensional Strongly-Correlated Systems (Ph.D. thesis), ETH Zürich, 2017.
[25] J. Cirac, D. Pérez-García, N. Schuch, F. Verstraete, Matrix product states and projected entangled pair states: Concepts, symmetries, theorems, Rev. Modern Phys. 93 (2021) 045003.
[26] G. Evenbly, Algorithms for tensor network renormalization, Phys. Rev. B 95 (2017) 045117.
[27] M. Hinczewski, A. Berker, High-precision thermodynamic and critical properties from tensor renormalization-group flows, Phys. Rev. E 77 (2008) 011104.
[28] Z.-C. Gu, X.-G. Wen, Tensor-entanglement-filtering renormalization approach and symmetry-protected topological order, Phys. Rev. B 80 (2009) 155131.
[29] M. Hauru, C. Delcamp, S. Mizera, Renormalization of tensor networks using graph-independent local truncations, Phys. Rev. B 97 (2018) 045111.
[30] G. Evenbly, G. Vidal, Tensor network renormalization, Phys. Rev. Lett. 115 (2015) 180405.
[31] S. Yang, Z.-C. Gu, X.-G. Wen, Loop optimization for tensor network renormalization, Phys. Rev. Lett. 118 (2017) 110504.
[32] M. Bal, M. Mariën, J. Haegeman, F. Verstraete, Renormalization group flows of hamiltonians using tensor networks, Phys. Rev. Lett. 118 (2017) 250602.
[33] C. West, A. Garcia-Saez, T.-C. Wei, Efficient evaluation of higher-order moments and cumulants in tensor network states, Phys. Rev. B 92 (2015) 115103.
[34] M.-C. Chang, M.-F. Yang, Magnetization plateau of the classical Ising model on the Shastry-Sutherland lattice: A tensor renormalization-group approach, Phys. Rev. B 79 (2009) 104411.
[35] L. Onsager, Crystal statistics. I. A two-dimensional model with an order–disorder transition, Phys. Rev. 65 (1944) 117–149.